

On the Paleostress Analysis Using Kinematic Indicators Found on an Oriented Core

Lucie Nováková*, Milan Brož

Institute of Rock Structure and Mechanics, Academy of Science of the Czech Republic, V Holešovičkách 41, 182 09, Prague

*Corresponding Author: lucie.novakova@irsm.cas.cz

Copyright © 2014 Horizon Research Publishing All rights reserved.

Abstract Paleostress analysis enables identification of stress history of a studied area. Reliable data are however necessary to get consistent results. Fault planes containing kinematic indicators have to be searched and recognized. If surface field survey is impossible, data are lacking, or deeper parts of a rock environment are being studied, boreholes can provide additional information. This paper is presenting review on paleostress analysis using core inspection data. Various aspects of the subject including kinematic data acquisition, core orientation, sampling bias, data processing, paleostress analysis and recent stress estimation are being outlined. The method is being demonstrated using case story based on borehole situated in Tisá Granite Massif, Czech Republic.

Keywords Paleostress Analysis, Borehole Core, Kinematic Indicators, Bias Sampling, Recent Stress

1. Introduction

Borehole cores provide unique insight into a subsurface rock environment. Cores can unearth various geological parameters including mineralogy, petrophysical and geomechanical characteristics, a degree of weathering and so on. Cores also often reveal a brittle deformation of the rock.

In general, brittle deformation is the reaction of a rock on the applied stress. Faults are weak zones in lithosphere where stress was relieved by movements. During faulting marks may form on fault planes documenting orientation and sense of the movement [1]. It is however to keep in mind the indicators are ambiguous sometimes. Doblas [2] classified movement indicating marks (so called kinematic indicators) into 11 principal groups using 61 criteria. Striation, steps and groves (Fig. 1) are amongst the most frequent kinematic indicators.

Sometimes it is possible to identify two or even three different sets of kinematic indicators on the very same plane (Fig. 2). Clearly, at least one set of the indicators was created by movement along predisposed fracture plane [3]. Two sets of the kinematic indicators also points out the fault plane was reactivated during another stress event and determine relative timing of the events.



Figure 1. Kinematic indicators on granite core samples, striation (on the left), steps (in the middle) and groves (on the right).



Figure 2. Two sets of mineral accretion steps on a fault plane.

In general, the responsible stress could be deduced from the observed deformation. The kinematic indicators are frequently used in delineation of stress condition of both large geological units [e.g. 4,5] and relatively small rock blocks [e.g. 6]. The inversion based on Wallace-Boot theorem [7] was introduced by [3]. Later, new methods were suggested (e.g. Multiple Inverse Analysis, The Gauss method) [8,9]. The paleostress analysis however suggests relative aging of stress events (of phases) only. Moreover the youngest identified phase could not be assumed corresponding to the actual stress conditions without additional independent approval. The in-situ stress determination techniques are often based on borehole data [see 10,11]. Therefore it is advantageous to combine paleostress analysis of core data and in-situ stress techniques.

2. Method

2.1. Core Orientation

First original orientation of the inspected core must be known. The core could be either collected with known orientation or oriented later., a mistaken orientation precludes a correct result [12].

Nowadays all major drill companies realize oriented coring. Various methods are employed to orientate the cylinder of core fully. The common core orienting methods use different core face marking or recording, mechanical and optical, systems to merge core gained in following runs. The oriented coring methods include the down-hole spear, Ezy-Mark, Ballmark, Reflex, Corpro Oriented and Corientiring systems. Simple method could be used for short cores in hard rocks even without special equipment for oriented coring. Oriented mark made before start of drilling on the core-to-be top might eventually allow orientation of the core later on. Fracture surface characteristics as well as fractures sub-parallel to the core enable fit core parts together. It is however obvious crushed zones or missing core preclude orientation of deeper parts.

Nelson et al. [13] and [12] pointed out potential problems

of the oriented coring methods. Equipment failure as well as human mistake might result in incorrect data. Orientation of the core should be both controlled during drilling and crosschecked after.

Unoriented cores can be oriented later as long as there is a depth scaling of the core and appropriate data were well-logged (or the borehole is still accessible). Acoustic borehole imaging, televiwer or oriented borehole optical camera can be used. Significant fractures enable core orienting if identified both on the core and in the borehole [14].

Regardless the orienting method it is useful to mark selected direction (for example north in vertical boreholes) as a line on the cylinder surface. This line keeps the core orientation as well as eases the following measurements. Line is usually complemented with arrows pointing to the borehole bottom.

2.2. Detailed Core Inspection

The oriented core is subjected to a detailed brittle tectonic inspection. Fault, joints and kinematic indicators are searched, measured and documented. Use of a magnifying glass is recommended to look for even the tiniest kinematic indicators because of limited fault plane area. Photo documentation is advantageous.

Various methods and tools can be deployed to measure observed brittle tectonics. Holcombe et al. [15] described two common ways of measurement procedure in oriented core. Reorienting the core in sand or a mechanical jig enables direct measurement of the structures using classic field outcrop techniques. This straightforward procedure provides clear easily understandable results without any subsequent processing. Moreover, no conversion is required for non-vertical boreholes. The alpha-beta-gamma measurement, on the other hand, is simple and rapid. Nevertheless, it is necessary to calculate real plunge and dip from measured data in non-vertical boreholes (Fig. 3). Software tools (e.g. GeoCalculator) can be employed [15].

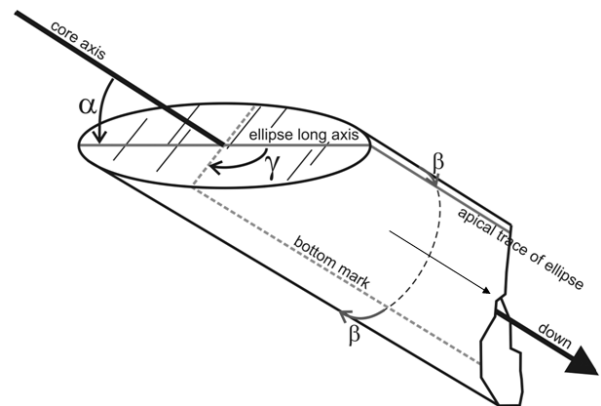


Figure 3. The alpha-beta-gamma method (after [15]).

Both methods mentioned above can be used to measure the observed kinematic indicators (lineation basically).

Sense of a movement documented by the kinematic indicators is highly important as well. In field, four basic types of the movement are being distinguished – strike-slip left or right lateral, normal and reverse fault. Level of uncertainty in the sense of movement determination should be recorded to avoid subjectivity (Tab. 1).

Table 1. Level of uncertainty in the sense of movement determination.

Quality factor	Uncertainty
0	Unknown
1	Sure
2	Probable
3	Supposed

Intersection law the most useful when relative age of two faults or kinematic indicators has to be set. Fault (indicator) cut by another fault (indicator) is older than the cutting one [16]. Again uncertainty has to be recorded and taken into account in later processing.

2.3. Sampling Bias Correction

Sampling bias has to be considered while studying brittle tectonics in boreholes. Hudson and Priest [17] suggested realization of tree boreholes with different orientation to get credible information. Maerz and Zhou [18] suggested optimisation of a borehole orientation for describing specific set of fractures. Linear sampling bias was introduced by [19]. Number of planar structures observed along a scan line (a borehole) depends also on the angle between the borehole and plane. Following equation describes the relation for infinite 2D fractures intersected by 1D scan line.

$$\frac{N}{L} = \frac{\sin \beta}{S},$$

where N is number of fractures intersected along the scan line, L stands for scan-line length, β represents minimum angle between the fracture and scan-line and S is fracture spacing in a direction perpendicular to the fracture set [19]. The fracture information in boreholes depends on the core diameter if the fracturing intensity profile along core is defined from fractures that essentially transect the core. The probability of intersecting a core depends on the distributions of both fracture lengths and orientations [20]. Specification is therefore necessary including borehole diameter D and size of a fracture H into equation [21,22]

$$\frac{N}{L} = \frac{\sin \beta}{S} + \frac{D}{S.H}.$$

Complete sampling bias correction is not trivial. Terzagi [19] suggested correction using weight $1/\sin \beta$. Terzagi correction overestimates fractures sub-parallel to the core. Priest [23] therefore limited the weight to 10 (cca 5.7°). Mauldon and Mauldon [24] introduced correction factors for boreholes according to diameter. Wang and Mauldon [25] derived proportional error the Terzagi correction and shadow

zone influence mathematically. Zetterlund and Ericsson [26] documented the Priest limitation could be insufficient for certain datasets. They promoted relative limitation instead. Any single fracture may not be responsible for more than 5-10% of total fracture count in the corrected dataset. In addition scale effect [see 27,28] a fracture characteristics distribution [20,29] have to be considered to reach universal solution in description of real discrete fracture network situation.

In practical terms linear sampling bias causes major complication because part of the fracture network could be easily missed out. The omission can cause misinterpretation when a set of fractures is omitted or one wide set of fractures appears like two [30]. Zetterlund and Ericsson [26] compared results of fracture mapping in on tunnel face, in borehole and using multiple 3D blocks. Both tunnel face mapping and borehole mapping missed one fracture set identified in 3D block data. The fracture mapping of tunnel faces identified almost same fracture sets as the boreholes did even though the scanlines along the boreholes were perpendicular to the tunnel faces. Paleostress analysis itself can be afflicted if the missed set bears unique kinematic information. Nováková et al. [14] showed paleostress analysis based on data collected in a quarry corresponds to the data found in a nearby borehole.

2.4. Paleostress Reconstruction

2.4.1. Paleostress Analysis

Since the 1970s a variety of methods have been proposed for estimating paleostress phases from field measurements of fault striations on fault planes [e.g. 8,9,31-33]. One of the best known and a widely used graphical technique to visualize paleostress phases is the Right Dihedra Method developed by [32]. This method is based on the idea that orientation of the maximum principal stress axis is constrained to the pressure quadrant (P), while orientation of the minimum principal stress axis is constrained to the tension quadrant (T) associated with a chosen fault. Spatial orientation and position of the P and T quadrants is defined by orientation of the fault plane and the slip direction along it. This enables to construct the approximate direction of the principal stresses as the geometrical centre of the common intersection of the P and T quadrants [34]. Existing methods can be roughly divided into two categories according to a data character. The first category assumes that the stress field is homogeneous [35,36]. The second category of the methods is concerned with heterogeneous sets of the field data [8,9,37].

2.4.2. Result Description

Detailed study of the fault structures on the borehole core and its interpretation provides the picture of the stress conditions within the studied borehole vicinity. The paleostress analysis results are three main directions of the stresses (σ_1 , σ_2 , σ_3), where σ_1 is the main direction of the

maximum principle stress, σ_2 is the main direction of the intermediate principle stress, σ_3 is the main direction of the minimum principle stress (Fig. 4) [34]. The easiest scheme is a stereogram with three various squares or circles, where the biggest one represents σ_1 , the middle one σ_2 and the smallest one σ_3 (Fig. 5). The other possible scheme of the studied fault planes might be a contour diagram showing the poles to the fault planes (Fig. 6). The density of contours is increasing with concentration of poles. This scheme is suitable for the determining prevailing directions of the fault planes and their directions.

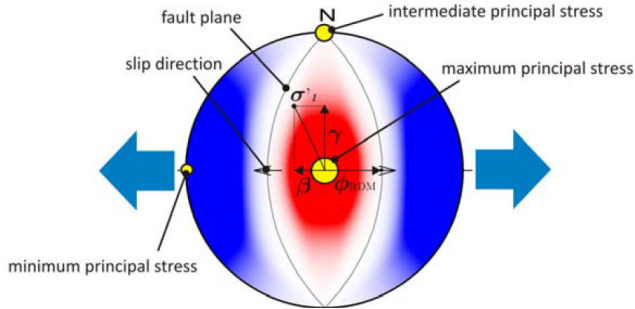


Figure 4. Directions of the principle stresses calculated by paleostress analysis [34].

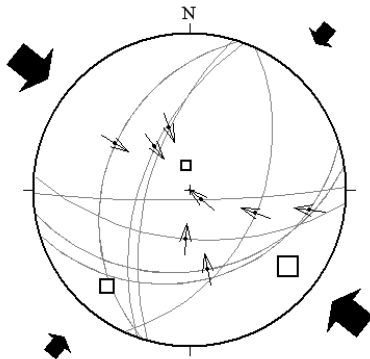


Figure 5. An example of the real paleostress conditions of the tectonic phase.

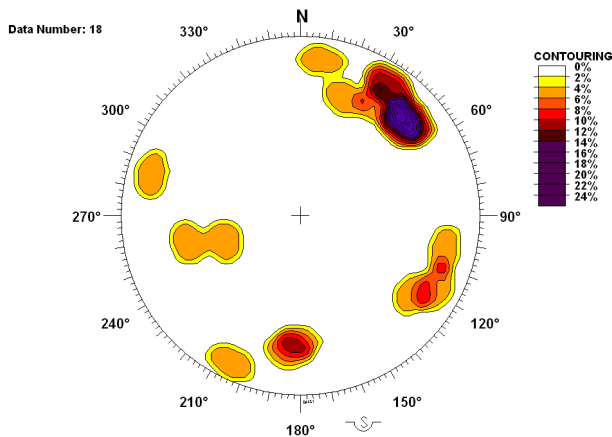


Figure 6. Contour diagram of the poles to the fault planes. Countouring interval 2%.

2.4.3. Recent Stress Determination

Even in cases with clear time succession of stress event paleostress analysis does not provide direct information about recent stress conditions. The phase identified as the youngest cannot be assumed contemporary. General stress trend can be deduced from World Stress Map [38]. Moreover several methods can be deployed to determine the recent stress [10,11]. The most common methods include the borehole breakout method [39,40] the overcoring method [41,42] and the hydraulic fracturing method [43]. In tectonically active areas, recent stress conditions can be also determined using earthquake focal mechanisms [44].

3. Case Story

The borehole TIV_1 has been drilled in 2011 in the Tisá Granite (part of the Čistá Massif) in the Czech Republic (Fig. 7). The borehole is 101 metres deep (Fig. 8). After the drilling, borehole acousting imaging has been done. We have identified 560 inhomogenities. The core has been studied very carefully and oriented using the results of BTV. Detailed structural geological research has been done on the borehole core. Strike and dip of the faults have been measured, as well as trend and plunge of the lineations occurring on the fault planes. The lineations were represented by kinematic indicators, mostly striations, calcite steps and asymmetric elevations. We have described the kinematic indicators (Fig. 9) their characteristics and relationships. We have found 27 fault planes with kinematic indicators (Tab. 2), in few cases, there were two sets of kinematic indicators on one fault plane. In these cases, it was possible to determine the relative age of crosscutting lineations. The fault planes were mostly subvertical to vertical striking NW-SE (Fig. 10).

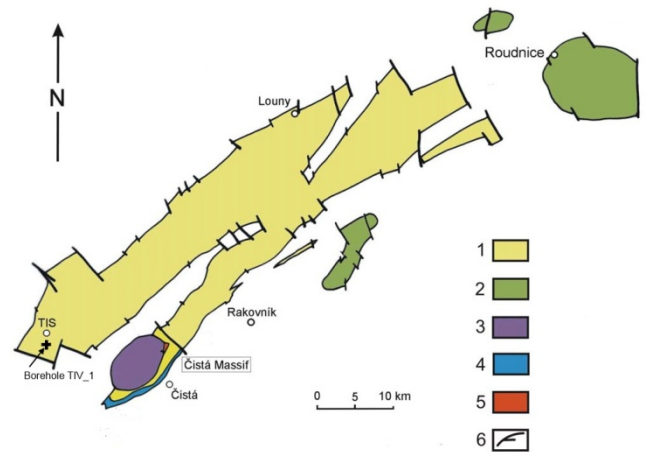


Figure 7. Schematic geological map with location of the borehole TIV_1. Legend: 1 – Tis Granite, 2 – Bechlín Diorite, 3 – Čistá Granodiorite, 4 – Černá Kočka Granite, 5 – Hürky Fenite, 6 – faults (after [45]).



Figure 8. The core of borehole TIV_1. Fault plane is marked by arrow.



Figure 9. Kinematic indicators on the borehole core TIV_1.

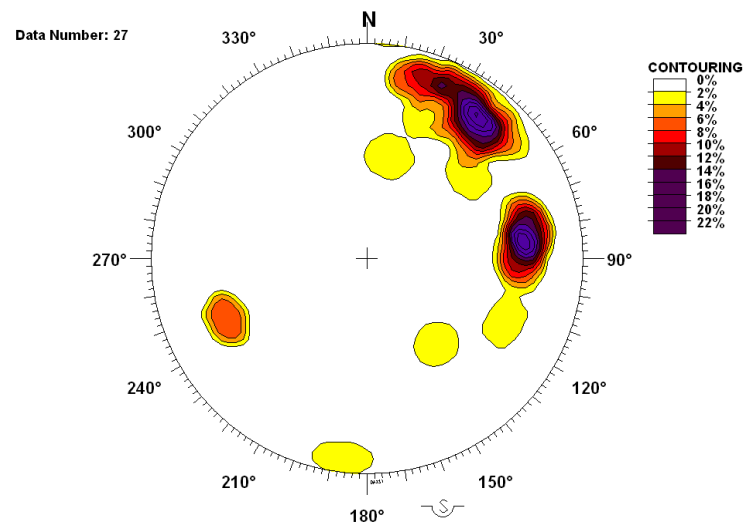
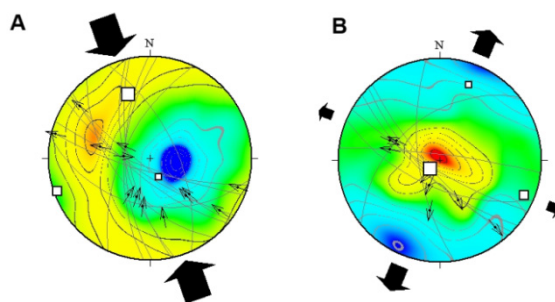


Figure 10. Contour diagram of poles to fault planes on the borehole core TIV_1. Contouring interval 2%.

Table 2. Fault planes and lineations on the borehole core TIV_1.

depth [m]	dip direction	dip	trend	plunge	quality	sense of movement
20.2	7	83	288	37	1	S
21.24	219	62	216	57	1	R
24.31	220	68	240	78	1	N
	220	68	313	9	1	D+N
28.21	228	76	143	9	2	S
29.32	321	43	294	35	2	N
29.93	214	72	119	9	1	D
31.42	210	78	312	5	1	S
	210	78	314	35	1	S+R
32.7	192	40	108	28	2	D
34.17	195	75	110	10	1	D
	195	75	282	2	1	D
66.97	262	66	340	27	2	D+N
	262	66	214	37	1	N+S
69.38	203	60	203	60	1	N
73.12	295	60	295	60	3	N
77.25	258	66	168	39	1	R+D
79.29	256	62	190	47	1	D+R
79.46	225	70	170	44	1	N
82.4	269	62	219	45	1	R
82.71	268	58	319	28	1	R
88.15	274	61	298	65	1	R
93.85	231	51	157	29	3	R
93.89	218	79	136	37	3	R
96.08	66	60	193	35	2	S+N
	66	60	208	50	1	R
98.44	201	79	286	37	1	D+N


Figure 11. Two tectonic phases calculated by paleostress analysis. A: older, B: younger.

Paleostress analysis of the fault-slip data based on the Gauss method [9] within the SMFZ resulted in identification of two tectonic phases. The phases have been ordered by the geological age on the base on the faults with multiple lineation systems and cross-cutting lineations on the fault planes. The relative age of the phases has been determined. The older phase represents mainly right-lateral faults. These faults were formed in the compressional regime with maximum compression (σ_1) in the NNW-SSE direction and minimum compression (σ_3) subvertical. The maximum compression axis is trending 341° and plunging 23° subhorizontally (Fig. 11A). The younger tectonic phase represents mainly normal faults. These faults were formed in the extensional regime with maximum extension (σ_1) in the subvertical direction and minimum compression (σ_3) in WNW-SES direction. The maximum compression axis is trending 226° and plunging 76° subvertically (Fig. 11B).

4. Concluding Remarks

Amongst other information detail inspection of core usually reveals brittle deformation of a rock environment. Oriented core is however essential when reconstructing stress conditions and tectonic history of a studied area. Several techniques can be employed to attain oriented core during drilling of oriented it later. Cross checking of core orientation is highly recommended.

It is not uncommon to identify kinematic indicators in core. Under near-surface conditions up to 27 kinematic indicators were found in 100 m long granite cores. Such dataset might provide reliable base for the paleostress reconstruction. Complexity and quality of a paleostress analysis depends on number, integrity and quality of data. Obviously the analysis cannot perform well in case just a few indicators were described. Generally, at least 10 kinematic indicators are required to get consistent analysis.

Sampling bias has to be considered when dealing with planar structures in boreholes. Fractures sub-parallel to the borehole can be easily missed. Shadow zone caused by the sampling bias affects the results and can confuse interpretation. Paleostress analysis is however less sensitive to the sampling bias in case of reactivation of perpendicular fracture typical for granite.

Paleostress analysis does not point out recent stress condition unreservedly. It is possible the youngest identified phase does not correspond to the current stress. Another method has to be applied if recent stress is studied. Several methods are ready to use in boreholes.

Acknowledgements

We are grateful to Ministry of Industry and Trade of the Czech Republic (Project Number: FR-TII/367) and Institute of Rock Structure and Mechanics (A VOZ30460519) for financial support and our colleagues from Arcadis Geotechnika Corp., Czech Geological Survey, ISATech, Ltd., Progeo Ltd., UJV Řež Corp. for fruitful project partnership.

REFERENCES

- [1] Hancock, P.L., 1985. Brittle microtectonics: principles and practise. *Journal of Structural Geology*, Vol. 7, 437–457.
- [2] Doblas, M., 1998. Slickenside kinematic indicators. *Tectonophysics*, Vol. 295, 187–197.
- [3] Angelier, J., 1979. Tectonic analysis of fault slip data sets. *Journal of Geophysical Research*, Vol. 89, No. B7, 5835–5848.
- [4] Bergerat, F., Angelier, J., Andereasson, P., 2007. Evolution of paleostress fields and brittle deformation of the Tornquist Zone in Scania (Sweden) during Permo-Mesozoic and Cenozoic times. *Tectonophysics*, Vol. 444, 93–110.
- [5] Lee, J.Ch., Lu, Ch.Y., Chu H.T., Delcaillau, B., Angelier, J., Deffontaines, B., 1996. Active Deformation and Paleostress Analysis in the Pakua Anticline Area of Western Taiwan. *TAO*, Vol. 7, No. 4, 431–446.
- [6] Havíř, J., 2002. Variscan and Post-Variscan Paleostresses on the Southeastern Margin of the Nížký Jeseník Region (Czech Republic). *Geolines*, Vol. 14, 33–34.
- [7] Bott, M.H.P., 1959. The mechanisms of oblique slip faulting. *Geological Magazine*, Vol. 96, 109–117.
- [8] Yamaji, A., 2000. The multiple inverse method: a new technique to separate stresses from heterogeneous fault-slip data. *Journal of Structural Geology*, Vol. 22, 441–452.
- [9] Žalohar, J., Vrabc, M., 2007. Paleostress analysis of heterogeneous fault-slip data: The Gauss method. *Journal of Structural Geology*, Vol. 29, 1798–1810.
- [10] Amadei, B., Stephansson, O. 1997. Rock stress and its measurement. Chapman & Hall (London). 490 pp.
- [11] Ljunggren, C., Changa, Y., Jansonb, T., Christiansson, R. 2003. An overview of rock stress measurement methods *International Journal of Rock Mechanics & Mining Sciences*, Vol. 40, 975–989.
- [12] Davis, B.K., Cowan E.J. 2012. Oriented Core - What the ... ? *Structural Geology and Resources 2012*, AIG conference paper.
- [13] Nelson, R.A., Lenox, L.C., Ward, B.J. Jr. 1987. Oriented core; its use, error, and uncertainty. *The American Association of Petroleum Geologist Bulletin*, Vol. 71, No.4. 357–367.
- [14] Nováková, L., Novák, P., Brož, M., Sosna, K., Pitrák, M., Kasíková, J., Rukavičková, L., Maňák, L. 2012. The Results of Borehole Acoustic Imaging from a Granite in the Jihlava District, Czech Republic: Implications for Structural Geological Research. *Journal of Geography and Geology*, Vol. 4, No. 4, 93–101.
- [15] Holcombe, R., Coughlin, T., Oliver, N. 2013. Oriented drillcore: measurements, conversion, and QA/QC procedures for structural and exploration geologists. *Oriented core manual*. HCO consultants.
- [16] Nováková, L., Hájek, P., Šťastný, M., 2010. Determining the relative age of fault activity through analyses of gouge mineralogy and geochemistry: a case study from Vápenná (Rychlebské hory Mts.), Czech Republic. *International Journal of Geosciences*, Vol. 1, No. 2, 66–69.
- [17] Hudson, J.A., Priest, S.D., 1983. Discontinuity frequency in rock masses *International Journal of Rock Mechanics and Mining Sciences & Geomechanics Abstracts*, Vol. 20, No. 2, 73–89.
- [18] Maerz, N. H., Zhou, W., 2000. Discontinuity data analysis from oriented boreholes. *Pacific Rocks; Proceedings of the Fourth North American Rock Mechanics Symposium*, Seattle, Washington, July 31- Aug.1, 2000, 667–674.
- [19] Terzaghi, R. D. 1965. Sources of error in joint surveys. *Geotechnique*, Vol. 15, 287–304.
- [20] Davy, P., Darcel, C., Bour, O., Munier, R., de Dreuzy, J.R.

2006. A note on the angular correction applied to fracture intensity profiles along drill core, *Journal of Geophysical Research*, Vol. 111.
- [21] Narr, W. 1996. Estimating average fracture spacing in subsurface rock. *AAPG Bulletin*, Vol. 80, No.10, 1565–1586.
- [22] Berg, C.R. 2012. The effect of fracture and borehole orientation on fracture frequency and density. RDA Dip Interpretation Suite tutorial. ResDip Systems.
- [23] Priest, S.D., 1993. *Discontinuity Analysis for Rock Engineering*, 1st Edn. Chapman & Hall, London, 473p.
- [24] Mauldon, M., Mauldon, J.G. 1997. Fracture Sampling on a Cylinder: From Scanlines to Boreholes and Tunnels. *Rock Mechanics and Rock Engineering*, Vol. 30, No.3, 129–144.
- [25] Wang, X., Mauldon, M., 2006. Proportional error of the Terzaghi correction factors. *Golden Rocks 2006, The 41st U.S. Symposium on Rock Mechanics (USRMS)*, June 17 - 21, 2006, Golden, CO, 6pp.
- [26] Zetterlund, M., Ericsson, L.O. 2012. Fracture mapping for geological prognoses. Comparison of fractures from boreholes, tunnel and 3-D blocks. *Eurock 2012 Proceedings*.
- [27] Berkowitz, B., Bour, O., Davy, P., Odling, N.E. 2000. Scaling of fracture connectivity in geological formations. *Geophysical Research Letters* Vol. 27, No. 14, 2061–2064.
- [28] Bonnet, E., Bour, O., Odling, N.E., Davy, P., Main, I., Cowie, P., Berkowitz, B. 2001 Scaling of fracture systems in geological media. *Reviews of Geophysics*, Vol. 39, No. 3, 347–383.
- [29] Marrett, R., Ortega, O.J., and Kelsey, C.M., 1999, Extent of power-law scaling for natural fractures in rock: *Geology*, Vol. 27, 799–802.
- [30] Martel, S.J., 1999. Analysis of Fracture Orientation Data From boreholes. *Environmental & Engineering Geoscience*, Vol. V, No. 2, 213–233.
- [31] Carey, E., Brunier, B., 1974. Analyse theorique et numerique d'un modele elementaire applique a l'etude d'une population de faille. *Comptes Rendus de l'Ycademie des Sciences, Paris, D*, Vol. 279, 891–894.
- [32] Angelier, A., Mechler, P., 1977. Sur une methode graphique de recherche de contraintes principales egalement utilisable et en seismologie: la methode des dièdres droits. *Bulletin Société Géologique de la France*, Vol. 19, 1309–1318.
- [33] Nemčok, M., Lisle, R.J., 1995. A stress inversion procedure for polyphase fault/slip data sets. *Journal of Structural Geology*, Vol. 17, 1445–1453.
- [34] Žalohar, J., 2009. T-TECTO 3.0 Professional Integrated Software for Structural Analysis of Fault-Slip Data, Introductory Tutorial, pp 56.
- [35] Angelier, J., 1984. Determination of the mean principle directions of stresses for a given fault population. *Tectonophysics*, Vol. 56, T17–T26.
- [36] Nieto-Samaniego, A.F., 1998. Stress, strain and fault patterns. *Journal of Structural Geology*, Vol. 21, 1065–1070.
- [37] Liesa, C.L., Lisle, R.J., 2004. Reliability of methods to separate stress tensors from heterogeneous fault-slip data. *Journal of Structural Geology*, Vol. 26, 559–572.
- [38] Heidbach, O., Tingay, M., Barth, A., Reinecker, J., Kurfeß, D., Müller, B. 2009. The World Stress Map based on the database release 2008, equatorial scale 1:46,000,000, Commission for the Geological Map of the World, Paris, doi:10.1594/GFZ.WSM.Map2009.
- [39] Zoback, M.D., Moos, D., Mastin, L.G., Anderson, R.N. 1985. Well bore breakouts and in situ stress. - *Journal of Geophysical Research*, Vol. 90, 5523–5530.
- [40] Tingay, M., Reinecker, J., Müller, B. 2008. Borehole breakout and drilling-induced fracture analysis from image logs. *World Stress Map Project guidelines*.
- [41] Staš, L., Knejzlík, J., Rambouský, Z. 2004. Development of conical probe for stress measurement by borehole overcoring method. *Acta Geodynamica et Geomaterialia*, Vol. 1, No. 4 (136), 93–98.
- [42] Reinecker, J., Stephansson, O., Zang, A. 2008. Stress analysis from overcoring data. *World Stress Map Project guidelines*.
- [43] Baumgartner, J., Rummel, F. 1989. Experience with “fracture pressurization tests” as a stress measuring technique in a jointed rock mass. *International Journal of Rock Mechanics and Mining Science & Geomechanics Abstracts*, Vol. 26, 661–671.
- [44] Dubiel R., Ciborek, A. 2004. Estimation of the local stress field using seismological data. *Acta Geodynamica et Geomaterialia*, Vol. 1, No. 1 (133), 41–45.
- [45] Kopecký, L., CHlupáčová, M., Klomínský, J., Sokol, A. 1997. The Čistá-Jesenice Pluton in Western Bohemia: Geochemistry, Geology, Petrophysics and Ore Potential. – *Sbor. geol. Věd, ložisk. Geol. Mineral.* 31, 97–126.